Catalysis Letters Vol. 102, Nos. 1–2, July 2005 (© 2005)
DOI: 10.1007/s10562-005-5196-4

A platinum–cobalt-loaded NaY zeolite membrane for nonoxidative conversion of methane to higher hydrocarbons and hydrogen

Xuehong Gu[a], Jian Zhang[a], Junhang Dong[a,*], and Tina M. Nenoff[b]

[a]*Engineering Department of Petroleum and Chemical , PRRC New Mexico Institute of Mining and Technology, 801 Leroy Place, Socorro, NM 87801, USA*

[b]*Chemical and Biological Technologies, Sandia National Laboratories, P.O. Box 5800, MS 0734, Albuquerque, NM 87185,, USA*

Received 9 December 2004; accepted 16 February 2005

Platinum–Cobalt-loaded NaY zeolite (Pt–Co/NaY) membranes were synthesized for continuous, single-step nonoxidative conversion of methane to higher hydrocarbons (C_{2+}) and hydrogen. During isothermal operation at 300 °C, CH_4 flowed on the feed side of the membrane whilst H_2 flowed through the sweep side of the membrane. The C_{2+} products formed continuously on the H_2 sweep side. The results indicate that the Pt–Co/NaY catalytic membrane can overcome the two-step limitation for nonoxidative CH_4 conversion.

KEY WORDS: Pt–Co/NaY; catalytic membrane; methane; nonoxidative conversion; single-step.

1. Introduction

Effectively converting methane to higher hydrocarbons (C_{2+}) and hydrogen is a challenging research topic with tremendous industrial interests since methane is renewable through bioprocesses. The transition metal-catalyzed nonoxidative CH_4 conversion to C_{2+} and H_2 may offer an alternative to oxidative methods because of its outstanding advantages of low reaction temperature, high selectivity, and zero CO_2-emission [1–4]. However, practical consideration of the nonoxidative system has been discouraged by the limitation of its two-step reaction. In the first step, CH_4 is decomposed on the metal surface into methyl radicals ($CH_{x(0\leq x\leq 3)}$) and hydrogen; in the second step, the chemisorbed CHx species are rehydrogenated and oligomerized into C_{2+} [5–9]. To thermodynamically favor the two reaction steps, a relatively high temperature and a CH_4 atmosphere are needed in the first step, while a low temperature and a H_2 sweep are required in the second step. Although recent research demonstrated that the two steps could be accomplished at a single temperature[6,7], they must be conducted in different atmospheres, requiring inefficient, discontinuous operations to switch the atmosphere in packed-bed reactors.

It was recently reported that the Pt–Co-loaded NaY zeolite performed better than Pt/NaY and Co/NaY single metal catalysts in terms of CH_4 chemisorption capacity [10–12]. The Pt–Co/NaY catalyst exhibited 100% conversion of the chemisorbed CH_x ($x \approx 2$) [13] with C_{2+} selectivity of 83.6% in the rehydrogenation step. The enhanced performance of the Pt–Co/NaY catalysts was attributed to the increased reducibility of Co ions in NaY and the synergistic effect of Pt–Co on the C–C bond formation during hydrogenation [12].

In this work, Pt–Co/NaY membranes were developed to overcome the two-step limitation of the nonoxidative CH_4 conversion. The Pt–Co bimetallic clusters were loaded inside the zeolite channels. In operation, CH_4 carried by Helium flowed on one side of the membrane (feed side) and meanwhile the H_2 diluted by Helium flowed on the other side (sweep side). The principle of CH_4 conversion through the catalytic membrane is proposed to have three basic steps as illustrated in figure 1: (1) decomposition of CH_4 on the CH_4 feed side surface, (2) surface diffusion of chemisorbed CH_x through the Pt–Co-loaded zeolite channels to the H_2 sweep side driven by the gradient of surface coverage, and (3) rehydrogenation of the CH_x species to form C_{2+} under H_2 sweep. A limited back diffusion of H_2 can maintain a low level of H_2 on the CH_4 feed side surface and inside the catalyst-loaded zeolite pores that suppresses deep dissociation of CH_x into inactive carbonaceous species and benefits the C_{2+} selectivity [13].

2. Experimental

2.1. Catalytic membrane synthesis and characterization

NaY zeolite membranes were synthesized on 1 1/8 inch.-diameter α-alumina discs, 2 mm thick and mean pore size of 0.15 μm, by a seeding-secondary growth approach [14]. The Y-type zeolite has an effective pore size of 7.4 Å before loading the metal catalysts. The membrane synthesis solutions had a molar composition of $1.0Al_2O_3$–$12.8SiO_2$–$17.0Na_2O$–$864{\cdot}2H_2O$.

---

* To whom correspondence should be addressed.
E-mail: jhdong@nmt.edu

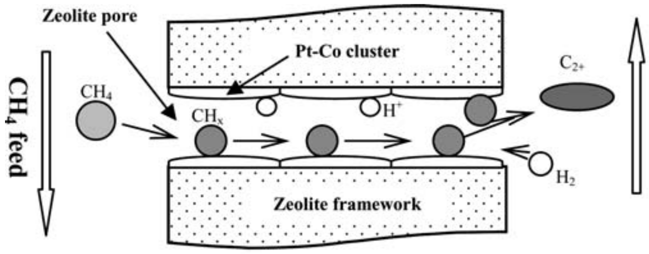

$$\left(\sum_{n=2}^{N} n\upsilon_n\right) CH_4 \xleftrightarrow{Pt\text{-}Co\ cat, \sim 300^\circ C} \sum_{n=2}^{N}(\upsilon_n C_n H_{2n+2}) + \left[\sum_{n=2}^{N}\upsilon_n(n-1)\right]H_2 + \Delta H_r$$

Figure 1. Schematic showing the principle of the proposed membrane process.

The Si/Al atomic ratio of the resultant zeolite membrane was about 1.74 as determined by X-ray fluorescence (XRF). At 25 °C, the NaY membranes used in this work exhibited CO_2/N_2 selectivity values greater than 30 with N_2 permeance of $\sim 2 \times 10^{-8}$ mol/m^2 s Pa for an equimolar mixture, which indicate excellent membrane quality[14].

The NaY membranes were loaded with metal by successive ion exchange in a 0.065 M $Pt(NH_3)_4(NO_3)_2$ solution and a 0.06 M $Co(NO_3)_2$ solution under refluxing at 80 °C, respectively. The ion exchange time was varied to control the Pt–Co loading level. After each step of ion exchange, the membrane was rinsed with DI water, dried, and then heated at 350 °C in air for 3 h. The membrane was then mounted in a stainless steel cell sealed with graphite gaskets and reduced under pure H_2 permeation at 350 °C for 8 h. Pt–Co/NaY particulate catalysts were also prepared under the same conditions and used in a packed-bed reactor for comparison.

It was found that the zeolite structure and the membrane microstructure were partially damaged when the load of Pt–Co was high. The XRD patterns of the NaY and Pt–Co/NaY membranes after reduction are shown in figure 2. The Pt and Co peaks were not distinguishable in the low-load membrane with 15 min of ion exchange time (denoted as M15) due to the minimal quantity and highly dispersed state of metals. In the high-load membrane (24 h of ion exchange time), the diffraction peaks of Y zeolite disappeared as also observed in the literature [15]. There were broad peaks of Pt but no well-defined diffraction peaks of cobalt found for the high-load membrane (figure 2). However, the base line developed a broad hump in the 2θ region of the Pt(111), Pt(200) and Co(111) peaks, suggesting that cobalt existed as highly dispersed atomic clusters. The catalyst load was (18Pt + 25Co) μmol/g-NaY for M15 and (220Pt + 250Co) μmol/g-NaY for the high load membrane as determined by XRF.

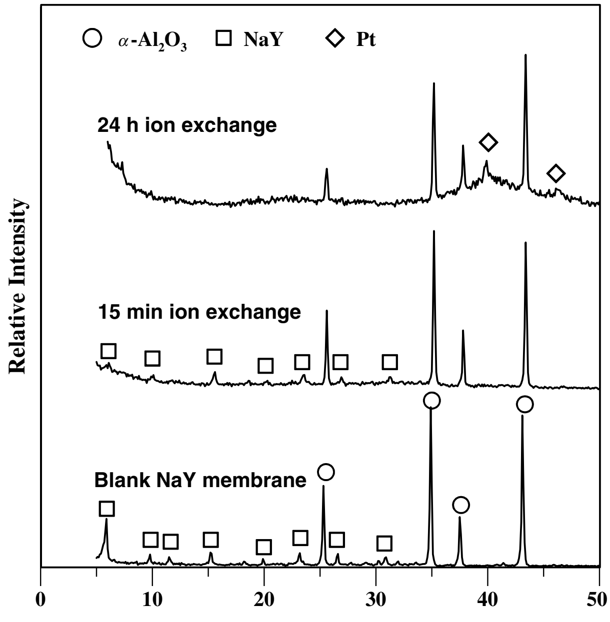

Figure 2. XRD patterns of the NaY and Pt–Co/NaY membranes.

The scanning electron microscopic (SEM) images of the Pt–Co/NaY membranes in (figure 3a and b) show micro-cracks formed in the high-load Pt–Co/NaY membrane that resulted from the structural destruction [15] and mismatch of thermal expansion between the zeolite and the alumina substrate [16]. Such a microstructural damage in the membrane was also evidenced by an unusually high N_2 permeance of nearly 10^{-6} mol/m^2 s Pa. The micro-cracks were not observed in the M15 (figure 3c and d), which had a low N_2 permeance of 8.14×10^{-9} mol/m^2 s Pa. The N_2 permeance data reported here were measured by steady state permeation of pure N_2 at 22 °C.

2.2. *Catalytic reaction*

All the gases used in the experiments had purities greater than 99.995% and were further treated by appropriate gas purifiers (Supelco Molecular Sieve 5A trap for methane and Supelpure-O columns for hydrogen and helium) before entering the reactors. C_{2+} was not detectable in the purified gases by the cryogenic condensation method used in this work. Liquid nitrogen cold traps were installed in both the feed and sweep outlet lines to collect the C_{2+} products, which were analyzed by a gas chromatograph (GC, HP 5890 II equipped with a Porapak © Q packed column and TCD detector). A mass spectrometer (MS, UTI 100C) was used to verify the product components. The experimental apparatus is schematically shown in figure 4.

Membrane M15 was tested for continuous isothermal CH_4 conversion at 300 °C and 0.86 bar. In the membrane reaction experiments, the feed stream was (8 cm^3 $CH_4 + 16$ cm^3 He)/min and the sweep stream was (4 cm^3 $H_2 + 10$ cm^3 He)/min. Under these conditions, the reaction was performed continuously for 5 h without membrane regeneration during the process. After the five-hour operation, the membrane was regenerated under pure H_2 (10 cm^3/min) flow on both sides at 300 °C for 1 h. The membrane reaction was then resumed with the same CH_4-feed stream, (8 cm^3 $CH_4 + 16$ cm^3 He)/min, but a new sweep flow of (2 cm^3 $H_2 + 10$ cm^3 He)/min to investigate the sweep side H_2 partial pressure on the CH_4 conversion.

For comparison with the catalytic membrane reactor, a packed-bed reaction of Pt–Co/NaY particulate catalyst, with the same metal loading as the membrane M15, was tested with the traditional two-step approach. Every cycle of the two-step reaction included three consecutive stages. First, the pure CH_4 was fed at a rate of 8 cm^3/min for 3 min. Second, pure helium was fed as a purge gas at 20 cm^3/min for 10 min. Third, pure H_2 was flowed through the packed-bed at 10 cm^3/min for 10 min.

3. Results and discussion

In both the catalytic membrane reaction and the packed-bed reaction, the major products were ethane and propane. Butane and pentane were evident in the

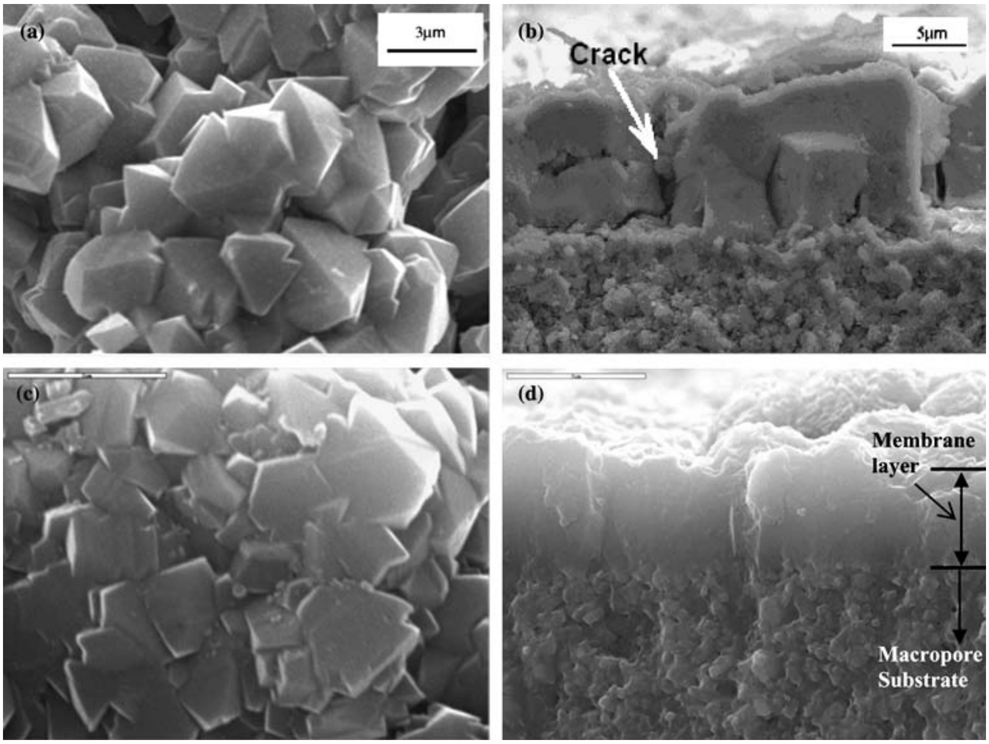

Figure 3. SEM images of The Pt–Co/NaY membranes. (a) surface and (b) cross-section: membrane by 24 h ion exchange; (c) surface and (d) cross-section: membrane by 15 min ion exchange.

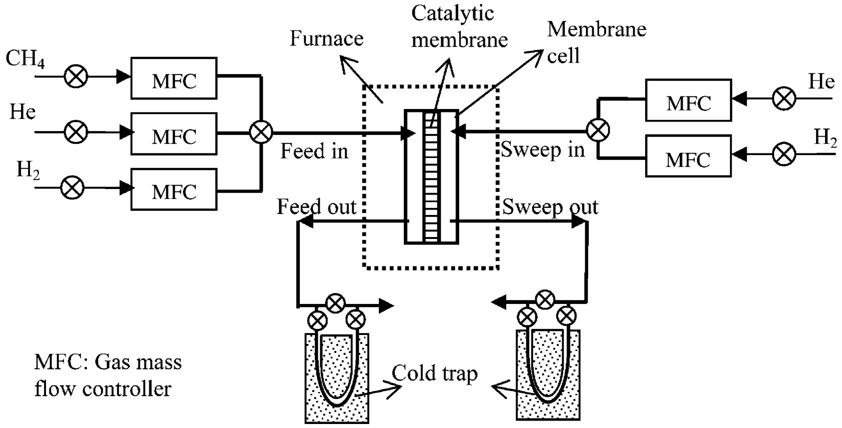

Figure 4. Schematic diagram of the membrane reactor system.

product but in minimal amounts. The amount of CH_4 converted to C_4 and C_5 was estimated to be in a range of 1–4% of the total CH_4 converted to C_{2+} based on GC detection. An accurate and quantitative measurement of C_4 and C_5 was difficult because of the extremely low concentration. Hydrocarbons heavier than C_5 were not evident even by MS detection. The absence of C_{5+} in this study was different from those reported in the literature where C_{5+} compounds were observed on the same type of catalysts [13]. This was likely caused by the different sample collection and analysis methods used in this work since such heavy compounds were extremely dilute in the product. Therefore, only C_2 and C_3 are included in the following discussions. The results of CH_4 conversion on M15 are presented in figure 5. The results of the packed-bed reaction with low-load Pt–Co/NaY particles are shown in figure 6 for comparison.

In the membrane process, C_{2+} were produced continuously, mainly on the H_2 sweep side. On the CH_4 feed side, a much smaller amount of C_{2+}, about 5% of that on the H_2 sweep side, was found because C_{2+} also formed during the CH_4 chemisorption step [13]. This demonstrated that the methyl radicals were generated on the CH_4 feed side or inside the Pt–Co loaded zeolite pores, diffused to the H_2 sweep side, and then rehydrogenated under the H_2 flow. The CH_x coverage on the membrane surface of the CH_4 feed side, where CH_x is formed, is higher than that on the membrane surface of the H_2 sweep side, where CH_x is consumed. Thus a CH_x gradient exists across the membrane thickness that drives the radical diffusion. However, the actual process of radical diffusion may be rather intricate because of the complexity of the CH_x–metal interactions [3] and the anticipated coinstantaneous CH_4 transport and H_2 back diffusion, which suppresses deep dissociation of CH_x into inactive carbonaceous species [13].

High H_2 sweep flow appeared to favor the selectivity of C_3H_8, which is consistent with the observation in the literature [13]. The C_{2+} productivity declined moderately with operation time. This is possibly due to the formation of less reactive carbonaceous species. The membrane could be effectively regenerated in pure H_2, indicating that no significant inactive carbon phase was formed. It was also found that C_{2+} production at 300 °C was three to four times that at 250 °C (data not shown here), which can be explained by the fact that CH_4 chemisorption and radical diffusion rates increase

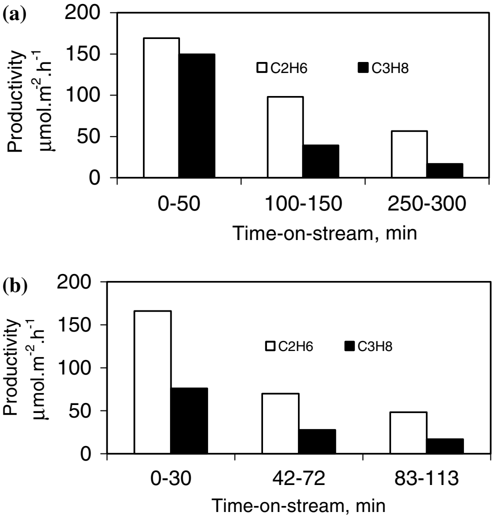

Figure 5. C_{2+} productivity of membrane M15 at 300 °C as a function of operation time. (a) Sweep stream (4 cm^3 H_2 + 10 cm^3 He)/min; (b) sweep stream (2 cm^3 H_2 + 10 cm^3 He)/min.

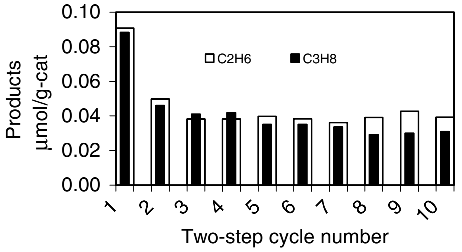

Figure 6. C_{2+} production at 300 °C by two-step reaction in the packed-bed reactor loaded with 200 mg of Pt-Co/NaY particles.

with increasing temperature. An additional experiment was conducted by adding the 4cm^3 H_2/min to the (8cm^3 CH_4 + 16cm^3 He/min) feed stream while sweeping with a pure He flow at 12cm^3/min. In this case, no production of C_{2+} was observed. This indicates that CH_4 conversion through the membrane can proceed only when the two sides of the membrane hold thermodynamically favorable atmospheres for the chemisorption and rehydrogenation steps, respectively.

The amount of catalyst on the M15 was estimated to be ~10 g-(Pt–Co/NaY)/m^2 based on the thickness of the membrane (~5 μm) and theoretical density of FAU zeolite (1.89 g/cm^3). As shown in table 1, with the same amounts of Pt–Co/NaY catalyst, the packed-bed needs to operate three cycles per minute to achieve the same productivity of the membrane reactor. These data further demonstrate that the catalytic membrane can overcome the two-step limitation and perform a truly continuous, single-step operation of nonoxidative CH_4 conversion. Ongoing studies are focusing on the optimization of the catalytic membrane, including catalyst loading levels and run temperatures. Until then we are not able to directly compare the membranes versus the packed bed reactor data.

4. Conclusion

A new type of Pt–Co/NaY catalytic membrane has been synthesized. Initial results confirm that the membranes have achieved a continuous, single-step isothermal operation for the two-step nonoxidative CH_4 conversion to C_{2+} and H_2. A three-step mechanism was proposed for the membrane reaction process, including (1) chemisorption of CH_4 on the feed side membrane surface to form $CH_{x(0\leq x\leq 3)}$ species, (2) diffusion of chemisorbed CH_x through the Pt–Co-loaded, subnanometer zeolite channels to the H_2 sweep side driven by the gradient of surface coverage, and (3) rehydrogenation and oligomerization of CH_x to form C_{2+} under H_2 sweep. Membrane synthesis and testing conditions are currently being optimized. The proof-of-concept of the novel catalytic membrane reported in this letter may open up new opportunities for research in related areas such as CH_4 conversion, membrane technology, surface science and catalysis.

Table 1

Relationship between the non-optimized 1-m^2 membrane reactor and a packed column with equivalent amount of Pt–Co/NaY catalyst (10 g)

Reaction time, (h)	Total CH_4 converted to C_{2+} on membrane[a]	Number of two-step cycles needed for packed-bed to produce equivalent C_{2+}
5	1910 μmol	893

[a] The regeneration time after the five-hour membrane reaction is not included.

Acknowledgments

The authors gratefully acknowledge the financial supports from the NELHA/DOE and NETL/DOE (DE-FC26-04NT15548). Sandia is a multiprogram laboratory operated by Sandia Corporation, a Lockheed Martin Company, for the U.S. DOE's National Nuclear Security Administration under contract DE-AC04-94AL85000.

References

[1] M. Belgued, P. Pareja, A. Amariglio and H. Amariglio, Nature 352 (1991) 789.

[2] T. Koerts and R.A. Vansanten, J. Chem. Soc. Chem. Commun. (1991) 1281..

[3] H. Amariglio, J. Saint-Just and A. Amariglio, Fuel Process. Technol. 42 (1995) 291.

[4] A.K. Kinage, R. Ohnishi and M. Ichikawa, Catal. Lett. 88 (2003) 199.

[5] T. Koerts, M.J.A.G. Deelen and R.A. Santen, J. Catal. 138 (1992) 101.

[6] M. Belgued, A. Amariglio, P. Paréja and H. Amariglio, J. Catal. 159 (1996) 44.

[7] Z. Hlavathy, Z. Paál and P. Tétényi, J. Catal. 166 (1997) 118.

[8] M.C. Wu and D.W. Goodman, J. Am. Chem. Soc. 116 (1994) 1364.

[9] T.V. Choudhary, E. Aksoylu and D.W. Goodman, Catal. Rev. 45 (2003) 151.

[10] L. Guczi, R.A. Santen and K.V. Sarma, Catal. Rev. 38 (1996) 249.

[11] L. Guczi, K.V. Sarma and L. Borkó, Catal. Lett. 39 (1996) 43.

[12] G.M. Lu, T. Hoffer and L. Guczi, Catal. Lett. 14 (1992) 207.

[13] L. Guczi and L. Borkó, Catal. Today 64 (2001) 91.

[14] X. Gu, J. Dong and T.M. Nenoff, Ind. Eng. Chem. Res., (2004) in press.

[15] B. Imre, I. Hannus, Z. Kónya and I. Kiricsi, J. Mol. Struct. 651 (2003) 191.

[16] J. Dong, Y.S. Lin, M.Z.C. Hu, R.A. Peascoe and E.A. Payzant, Micropor. Mesopor. Mater. 34 (2000) 241.